

Enhancement in above-threshold ionization spectrum

Guanghan Ge^a, Xiaohong Song^{a,*}, Jing Chen^{b,c,*}, and Weifeng Yang^{a,*}

Received: May 3, 2017,
Accepted: June 16, 2017,

DOI: 10.4208/jams.050317.061617a

<http://www.global-sci.org/jams/>

Abstract. Freeman resonance and resonance-like enhancement (RLE) in above-threshold ionization (ATI) spectrum are reviewed in this work. Two different interpretations accounting for the high-energy enhancements in the ATI spectra are described. One of them is the multiphoton ionization “channel closing” relating to the destructive/constructive interference, while the other pursue the fundamental concept of resonance and associates the enhancement with a resonant excited state. Primary calculation of the RLE using generalized quantum trajectory Monte Carlo method is also present.

1. Introduction

Above-threshold ionization (ATI), which was firstly observed in 1979 [1], has been identified as the core of strong-field physics and the most important process in the interaction between atoms and intense laser field. ATI is the process that an atom in an intense laser field absorbs s more photons than the minimum number n for reaching to the ionization threshold I_0 . The ionization peaks separated by the energy of one photon are present in ATI spectra. The energies of the ATI peaks are given by

$$E=(n+s)\omega-I_0. \quad (1)$$

Freeman resonance was found in experiment thirty years ago [2], and sub-peaks associated with certain excited states being resonant with the ground state are shown in the low-energy part of the ATI spectra. If the photoelectron does not interact with the parent ion after it is born in the field, the gaining energy of it cannot exceed $2U_p$ ($U_p=I/4\omega^2$ denotes the ponderomotive energy, where I is the laser intensity and ω is the angular frequency). In the energy region higher than $2U_p$, the rescattered photoelectrons are dominated and the electron spectrum shows a plateau. After the observation of Freeman resonance, the magnitudes of peaks in the high-energy ATI spectra around $5\sim 10U_p$ were found to exhibit strong variations when the laser intensity changes slightly [3][4]. Since the low-energy enhancement mechanism is reminiscent of the excited state resonances, the enhancement in high-energy region is attributed to the Rydberg resonances. Numerical solution of time-dependent Schrödinger equation (TDSE) well reproducing the ATI spectra [5][6][7], confirmed that the rescattering of electron wave packet from excited state leads to the enhancement feature [5].

However, opposing strong-field approximation (SFA) calculations with a zero-range potential, for which no excited state exist, can also reproduce the enhancements in the plateau [8][9][10]. This is interpreted in terms of the constructive interference of quantum trajectories when n -

photon ionization channel is closing. To contribute to the debate of the two contradicting interpretations, intensity-dependent ATI spectra in the direction of the polarization and those in the direction perpendicular to the polarization are compared, supporting the latter [11]. On the other hand, TDSE calculations with a long-range potential confirm that the enhancement in the high-energy part of ATI spectra originates from multiphoton resonance between the ground state and Rydberg states, and laser-induced states were proposed instead of ruling out the validity of channel closing [12]. Very recently, experiments on strong-field excitation together with TDSE calculations try to combine the seemingly opposing pictures, i.e., channel closing and rescattered electron's resonances with Rydberg states [13].

While the enhancement in the high-energy ATI spectra of rare-gas atoms do not have a unified theoretical interpretation yet, experimental observations of such enhancements were reported in simple molecules [14][15]. Recently, the enhancement of polyatomic molecules was observed [16][17]. Theoretical calculations using the SFA reproduced the experimental results and attributed the different characteristics of different molecules to interference effects of molecular orbitals with different symmetries [16], which, in fact, supported the channel closing mechanism.

In this paper, we will describe the enhancement both in low-energy and high-energy parts of the ATI spectra. The two distinct interpretations accounting for enhancement of the ATI peaks in the high-energy part of ATI spectra will be reviewed. Recent progress and applications in resonance structures will be introduced.

2. Freeman resonance

In this section, we first look back on the Freeman resonance [2], and then introduce the observation of Freeman resonance delay between the photoelectrons emitted via the field-dressed Rydberg states [18].

2.1. Freeman resonance

Figure 1 shows the first measurements of Freeman resonance [2]. When the pulse duration is less than 1 picosecond (ps), the peaks in low-energy part of ATI spectra break up into a series of narrow peaks. For long pulses, the ponderomotive energy of the photoelectron when it exits form the interaction volume counteracts the decreased kinetic energy due to the raised ionization potential. Therefore, it is impossible to find the shift

^a Department of Physics, College of Science, Shantou University, Shantou, Guangdong 515063, China.

^b HEDPS, Center for Applied Physics and Technology, Peking University, Beijing 100084, China.

^c Institute of Applied Physics and Computational Mathematics, P. O. Box 8009, Beijing 100088, China.

* Corresponding author, songxh@stu.edu.cn

* Corresponding author, chen_jing@iapcm.ac.cn

* Corresponding author, wfyang@stu.edu.cn

effect of ionization potential with long pulse. When the pulse duration is short enough, there is no time for the escaped photoelectron to accelerate and the spectrum faithfully records the photoelectron energies and momentum distributions at the moment of ionization. Excited states of atom shift upward along with the ionization potential by U_p . The energy shift of an intermediate bound state is

$$E = (n+s)\omega - I_0 - (m\omega - E_i), \quad (2)$$

where E_i is the original energy of the state and m is the number of photons resonant with the state. The fine structure and the corresponding ATI peaks of Freeman resonance are shown in Fig. 2 [2].

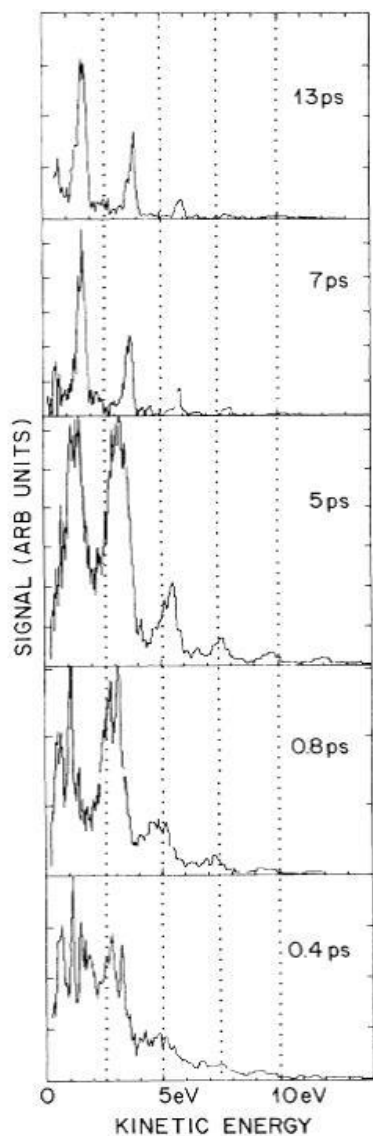


Figure 1: Kinetic energy of photoelectrons emitted from xenon as a function of pulse width. The intensity increases from $1.2 \times 10^{13} \text{ W/cm}^2$ for pulse width 15 ps to $3.9 \times 10^{14} \text{ W/cm}^2$ for 0.4 ps (adapted from Ref. [2]).

2.2. Attosecond time delay of Freeman resonance

In this subsection, we will introduce the recent measurements of attosecond time delay of Freeman resonance. A phase-controlled orthogonal two-color (OTC, 800-400nm) femtosecond laser pulse was employed to probe the photoelectron emission delay in multiphoton ATI of an atom [18]. Figure 3 shows the measured, the generalized quantum

trajectory Monte Carlo (GQTM) [20] and the TDSE ϕ_L -integrated (ϕ_L is the relative phase of the OTC pulse) photoelectron angular distributions of singly ionized argon (Ar). Along y -axis ($\phi_e = 0^\circ$ or $\pm 180^\circ$, ϕ_e is the emission angle of the electron) only main ATI peaks (labeled by white dots) spaced by 400nm photon energy is observed. Additional sidebands differed by a photon energy of the 800nm field between two adjacent main ATI peaks appear for electrons emitted away from the y -axis, e.g. $\phi_e = 30^\circ$ (labeled by black dots).

The GQTM simulations, which have well reproduced different experimental and TDSE results with different parameters [21][22][23], agreed with the experimental observations here (see Fig. 3(a) and (b)). The Freeman resonance is not able to be included in the GQTM simulations without considering excited states. While other processes, such as the time delay induced by the multiphoton transition process and the free electron propagation in the combined field of the atomic potential and the laser field, can be described accurately. To estimate the Freeman resonance delay we ran the TDSE simulations [24][25][26] (see Fig. 3(c)) in parallel to the GQTM simulations. The Freeman resonance delay is revealed by subtracting the phase difference between the experimental measurements (or TDSE) and GQTM simulations. We observed a $(0.19\pi + 0.22\pi)/2 = 0.21\pi \approx 140$ attoseconds difference of time delay of photoelectrons emitted via the field-dressed Freeman resonant $4f$ and $5p$ Rydberg states of Ar. We summarize the experimentally measured and simulated phase differences between two photoionization pathways in Table 1. The data in the two rows corresponds to electrons emitting to $\phi_e = 0^\circ$ and $\phi_e = 30^\circ$.

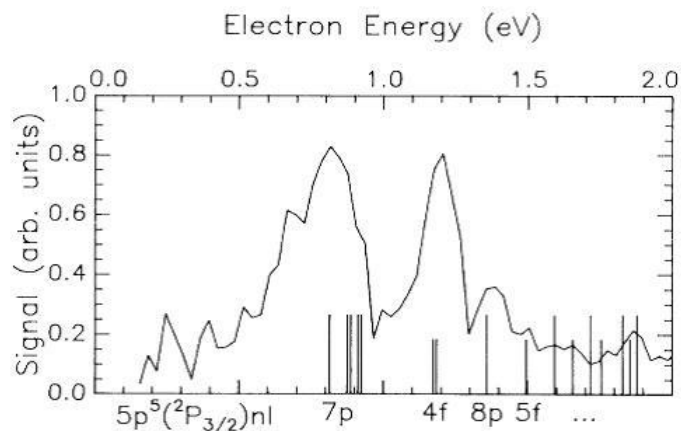


Figure 2: $s=0$ fine-structure data for pulse width less than 0.5 psec: also plotted is the location, according to Eq. (3), of the relevant $5p^5(2p_{3/2})nl$ states from Moore (Ref. [19]). The instrument resolution, which increases as the square root of the energy, is 0.05 eV at 0.5 eV and 0.1 eV at 2.0 eV. With the exception of the missing peak corresponding to the $5p^5(2p_{3/2})10p$ (1.72 eV) state, the experimental spectrum is reasonably well assigned above 0.8 eV. As discussed in the text, the peak in the spectrum below 0.8 eV may have their origin in the blend of a large number of states, including $m=5$ odd-parity resonances (adapted from Ref. [2]).

Table 1: Experimentally measured and simulated phase differences between two photoionization pathways, i.e. photoelectrons emitted via the $4f$ and $5p$ states of Ar (adapted from Ref. [18]).

Emission angle	Experiment	TDSE	GQTM	Freeman resonance delay difference	
				Exp.-GQTM	TDSE-GQTM
ϕ_e	$ \Delta\phi_{pp}^{exp} - \Delta\phi_{pp}^{tdse} $	$ \Delta\phi_{pp}^{tdse} - \Delta\phi_{pp}^{gqtm} $	$ \Delta\phi_{pp}^{gqtm} - \Delta\phi_{pp}^{exp} $	$\Delta\phi_{pp}^{4f/5p} = \Delta\phi_{pp}^{exp} - \Delta\phi_{pp}^{gqtm} $	$\Delta\phi_{pp}^{4f/5p} = \Delta\phi_{pp}^{tdse} - \Delta\phi_{pp}^{gqtm} $
0°	0.24π	0.19π	0.05π	0.19π	0.14π
30°	0.42π	0.33π	0.20π	0.22π	0.13π